Relationship between water and aragonite barium concentrations in aquaria reared juvenile corals

Meagan Eagle Gonneea [a,*,1], Anne L. Cohen [b], Thomas M. DeCarlo [c,2], Matthew A. Charette [d]

[a] Woods Hole Coastal & Marine Science Center, U.S. Geological Survey, 384 Woods Hole Rd., Woods Hole, MA 02543, USA
[b] Department of Marine Geology & Geophysics, Woods Hole Oceanographic Institution, 266 Woods Hole Rd., Woods Hole, MA 02543, USA
[c] ARC Centre of Excellence for Coral Reef Studies, School of Earth Sciences and Oceans Institute, The University of Western Australia, Crawley, WA, Australia
[d] Department of Marine Chemistry & Geochemistry, Woods Hole Oceanographic Institution, 266 Woods Hole Rd., Woods Hole, MA 02543, USA

Abstract

Coral barium to calcium (Ba/Ca) ratios have been used to reconstruct records of upwelling, river and groundwater discharge, and sediment and dust input to the coastal ocean. However, this proxy has not yet been explicitly tested to determine if Ba inclusion in the coral skeleton is directly proportional to seawater Ba concentration and to further determine how additional factors such as temperature and calcification rate control coral Ba/Ca ratios. We measured the inclusion of Ba within aquaria reared juvenile corals (*Favia fragum*) at three temperatures ($\sim$27.7, 24.6 and 22.5 °C) and three seawater Ba concentrations (73, 230 and 450 nmol kg^{-1}). Coral polyps were settled on tiles conditioned with encrusting coralline algae, which complicated chemical analysis of the coral skeletal material grown during the aquaria experiments. We utilized Sr/Ca ratios of encrusting coralline algae (as low as 3.4 mmol mol^{-1}) to correct coral Ba/Ca for this contamination, which was determined to be 26 ± 11% using a two end member mixing model. Notably, there was a large range in Ba/Ca across all treatments, however, we found that Ba inclusion was linear across the full concentration range. The temperature sensitivity of the distribution coefficient is within the range of previously reported values. Finally, calcification rate, which displayed large variability, was not correlated to the distribution coefficient. The observed temperature dependence predicts a change in coral Ba/Ca ratios of 1.1 µmol mol^{-1} from 20 to 28 °C for typical coastal ocean Ba concentrations of 50 nmol kg^{-1}. Given the linear uptake of Ba by corals observed in this study, coral proxy records that demonstrate peaks of 10–25 µmol mol^{-1} would require coastal seawater Ba of between 60 and 145 nmol kg^{-1}. Further validation of the coral Ba/Ca proxy requires evaluation of changes in seawater chemistry associated with the environmental perturbation recorded by the coral as well as verification of these results for *Porites* species, which are widely used in paleo reconstructions.
Published by Elsevier Ltd.

Keywords: Coral Ba/Ca; Barium; Aragonite; Distribution coefficient; *Favia fragum*

---

* Corresponding author.
E-mail addresses: mgonneea@usgs.gov (M.E. Gonneea), acohen@whoi.edu (A.L. Cohen), thomas.decarlo@uwa.edu.au (T.M. DeCarlo), mcharette@whoi.edu (M.A. Charette).
[1] Formerly at, Department of Marine Chemistry & Geochemistry, Woods Hole Oceanographic Institution, 266 Woods Hole Rd., Woods Hole, MA 02543, USA.
[2] Formerly at, Department of Marine Geology & Geophysics, Woods Hole Oceanographic Institution, 266 Woods Hole Rd., Woods Hole, MA 02543, USA.

1. INTRODUCTION

Coral inclusion of barium (Ba) has been linked to changes in ocean chemistry with variability in coral Ba/Ca implicated as a climate proxy of river discharge, river sediment transport, upwelling, and groundwater discharge (itself a rainfall proxy) (Table 1 and references therein). Reconstruction of such environmental records provides valuable insight into past climate conditions. The utility of the coral Ba/Ca proxy stems from several factors. First, Ba readily substitutes for Ca within the aragonite skeleton due to similar ionic radii. Second, terrestrial water and sediment sources have elevated Ba compared to seawater (Gaillardet et al., 2003; Shaw et al., 1998). Finally, the temperature dependent partitioning of Ba between inorganic aragonite and fluid has been determined experimentally

Table 1
Coral Ba/Ca environmental proxy studies.

Reference	Ba/Ca baseline (μmol mol^{-1})	Ba/Ca peak (μmol mol^{-1})	Proxy	Species	Location
Jupiter et al. (2008)	3.5	7	River	*Porites*	Round Top island, Great Barrier Reef
	4	6	River	*Porites*	Keswick Island, Great Barrier Reef
	3	8	River	*Porites*	Scawfell Island, Great Barrier Reef
Prouty et al. (2010)	3.4	8.0	Sediment	*P. lobata*	Kamalo, Molok'a Reef, Hawaii
	5.5	10.2	Sediment	*P. lobata*	One Ali'i, Molok'a Reef, Hawaii
	2.8	21.6	Sediment	*P. lobata*	Umpipa'a, Molok'a Reef, Hawaii
	3	17.8	Sediment	*P. lobata*	Pala'au, Molok'a Reef, Hawaii
Wyndham et al. (2004)	4	15	Unknown	*Porites*	Havannah Island, Great Barrier Reef
	4	15	Unknown	*Porites*	Pandora Reef, Great Barrier Reef
McCulloch et al. (2003)	4	12	River	*Porites*	Havannah Island and Pandora Reef, Great Barrier Reef
Reuer et al. (2003)	4.7	5.7	Upwelling	*Montastrea annularis*	Isla Tortuga, Venezuela
Sinclair and McCulloch (2004)	4	12	River	*Porites*	King Reef, Great Barrier Reef
	4	17	River	*Porites*	Pandora Reef, Great Barrier Reef
Chen et al. (2011)	6	15	Physiological	*Porites*	Daya Bay, South China Sea
	6	15	Physiological	*Porites*	Daya Bay, South China Sea
Fleitmann et al. (2007)	4	50	River/ sediment	*Porites*	Kenya
	4	9.5	River/ sediment	*Porites*	Kenya
Sinclair (2005)	4	13	Unknown	*Porites*	Cow Island, Great Barrier Reef
	4	12	Unknown	*Porites*	Orpheus Island, Great Barrier Reef
Alibert et al. (2003)	4.5	14	River	*Porites*	Pandora Reef, Great Barrier Reef
	3	6	River	*Porites*	Davies Reef, Great Barrier Reef
Montaggioni et al. (2006)	4.3	21	Upwelling	*P. lobata*	Amedee Islet, New Caledonia
	1.3	5.2	River	*P. lobata*	Vata Ricaudy Reef, New Caledonia
Lea et al. (1989)	4.1	5.1	Upwelling	*Pavona clavus*	Galapagos Islands
Alibert and Kinsley (2008)	4	25	Upwelling	*Porites*	New Ireland, Papua New Guinea
Carriquiry and Horta-Puga (2010)	7.5	9.3	River	*Montastraea faveolata*	Anegada de Adentro Reef, Veracruz Reef System, Gulf of Mexico
	7.5	9.3	River	*M. Faveolata*	Isla Verde, Veracruz Reef System, Gulf of Mexico
Horta-Puga and Carriquiry (2012)	4.7	7.5	Groundwater	*M. annularis*	Cancun, Mexico
	4.3	5.6	Groundwater	*M. annularis*	Cancun, Mexico
Fallon et al. (1999)	3.9	5.1	Upwelling	*P. lobata*	Shirigai Bay, Japan
Moyer et al. (2012)	3.3	4.8	River	*M. Faveolata*	Fajardo Puerto Rico
Tudhope et al. (1996)	5	15	Upwelling	*Porites*	Marbat, Oman, Red Sea
	3	6	Upwelling	*Porites*	Wadi Ayn, Oman, Red sea

(Dietzel et al., 2004; Gaetani and Cohen, 2006). Indeed, variability in coral Ba/Ca ratios typically cannot be explained by temperature changes alone, indicating additional influences. However, several studies report coral Ba/Ca ratios that did not vary in concert with a known driver. For example, Tudhope et al. (1996) and Sinclair (2005) reported elevated coral Ba/Ca that did not correlate to known upwelling or river runoff sources. Such uncertainty highlights the need to better understand the origin of coral Ba/Ca as an environmental proxy.

Coral Ba/Ca-based climate records are typically constructed by regressing coral Ba/Ca against a measure of the parameter of interest (e.g. river discharge or water temperature or nutrients as a proxy for upwelling) with the underlying assumption that variability in the Ba/Ca of the coral skeleton reflects changes in seawater chemistry caused by variability in the environmental driver (Table 1). In order for this assumption to be true, the following conditions have to be met: first, temperature driven changes in coral Ba/Ca should be insignificant compared to the other driver of the Ba/Ca signal, or can be adequately corrected for; second, seawater Ba/Ca should increase in direct proportion to the proposed driver (i.e. terrestrial input, river flow, and groundwater discharge); and third, corals should incorporate the seawater Ba/Ca signal in a predictable fashion.

To gain a mechanistic understanding of the Ba/Ca coral proxy and test the three conditions listed above, we grew *Favia fragum* coral polyps in seawater amended with Ba at three different concentrations and three different temperatures to quantify solid-solution Ba partitioning as a function of temperature, calcification rate, aragonite saturation state, and seawater Ba concentration.

2. METHODS

2.1. Experimental conditions

The coral culture experiments were performed at the Bermuda Institute of Ocean Sciences (BIOS) in July 2011. Nine aquaria (20 L) were established in three different temperature controlled (~27.7, 24.6 and 22.5 °C) and Ba-amended (73, 230 and 450 nmol kg^{-1}) baths such that each tank had a different combination of temperature and Ba concentration (Table 2). These Ba concentrations are well below the saturation state of witherite (BaCO$_3$) (log equilibrium constant = −8.57 (Busenberg and Plummer, 1986), experiment log solubility product = −10.0 to −10.9). Sea water was supplied from the lagoon adjacent to BIOS through a seawater intake and had an ambient temperature of 27 °C and Ba concentration of 44 nmol kg^{-1}. Temperature was monitored in all but one of the tanks with Onset™ HOBO water temperature loggers and the three tanks at each temperature treatment shared a water bath. Ambient CO$_2$ conditions were maintained by directly bubbling air through micropore bubble 'wands' attached at the base of each aquarium thereby maintaining a stable aragonite saturation state; this also served to keep the tanks well mixed. The tanks were drained and refilled with filtered seawater (5 µm) at the beginning of the experiment and then on days

5 and 11 to prevent the buildup of nutrients during the 14-day experiment. Once the tanks were filled, they were amended with a dissolved Ba standard (a high purity BaCO$_3$ dissolved in 0.11% nitric acid, Fluka® Analytical). Samples for salinity, trace element content, total alkalinity (TA), and dissolved inorganic carbon (DIC) were collected at the beginning and end of the experiment, as well as prior to each water change and after the element addition had equilibrated in the tank for one hour (a total of 8 measurements of water chemistry in each tank during the course of the experiment). Some evaporation was observed despite plastic covering on the aquaria, which likely explains the range in salinities and water chemical properties observed among different tanks over time (Table 2 and Supplemental Table 1).

2.2. Coral culture

Mature adult *F. fragum* colonies were collected from nearby reefs 3 to 5 days prior to the July spawn (Goodbody-Gringley and de Putron, 2009). They were kept in outdoor flow-through aquaria during the day and isolated at night. Zooxanthellate larvae were collected each morning, and then added to plastic containers with mesh tops containing ceramic tiles (de Putron et al., 2011). These tiles were preconditioned for larval recruitment by placing them on the nearby reef for several months prior to use. During this time, encrusting coralline algae (hereafter CCA) and other algal growth was established on the tiles. Some CCA and algal growth was removed from the tile prior to use in the experiment, thus CCA growth occurred during pre-conditioning on the reef as well as in controlled aquaria conditions. The larvae were then allowed to settle on these tiles in aquaria established at experimental conditions for 48 h to encourage coral planulae to attach to the tiles and metamorphose into polyps, at which point calcification of the coral skeleton begins. At this point, the tiles were removed from the mesh-topped containers and placed directly in the aquaria. Each day, light levels were maintained for 12 h at 215 ± 59 µmol quanta m^{-2} s^{-1} (± indicates one standard deviation throughout). The polyps were allowed to grow for 14 days, after which the polyps were removed from the aquaria, rinsed with a 5% bleach solution to remove organic material, subsequently rinsed with deionized water, and dried (Drenkard et al., 2013).

2.3. Analytical methods

Tank salinity was measured at BIOS with an Autosal salinometer. The alkalinity and dissolved inorganic carbon samples were poisoned with mercuric chloride immediately after collection and analyzed using a Marianda VINDTA-3C analysis system at Woods Hole Oceanographic Institution. Total alkalinity was determined by non-linear curve fitting of data obtained by open-cell titrations and DIC concentrations were determined by coulometric analysis. The pCO_2 and aragonite saturation state were calculated from discrete tank temperature, salinity, TA, and DIC samples using the CO2SYS program (Lewis and Wallace, 1998;

Table 2
Aquaria experimental conditions, dissolved Ba, coral precipitation rate, solid Ba/Ca and Sr/Ca and K_{Ba}.

Tank#	Salinity ± SD	Temperature (°C ± SD)	CO_2 (ppmv ± SD)	Ω_{AR} (±SD)	[Ba] (nmol kg^{-1} ± SD)	Dissolved Ba/Ca (μmol mol^{-1} ± SD)	Calcification rate (mg d^{-1} ± SD)	Solid Ba/Ca (μmol mol^{-1} ± SD)[b]	Solid Sr/Ca (mmol mol^{-1} ± SD)	K_{Ba}[b]	Individuals/ Measurements[c]
1: coral	34.7 ± 1.1	27.7 ± 0.9	320 ± 50	3.2 ± 0.3	79 ± 23	7.5 ± 2.0	6.2 ± 4.2	12.1 ± 1.6	8.2 ± 0.6	1.62 ± 0.21	43/24
2: coral	34.9 ± 1.1	27.8 ± 1.0	320 ± 30	3.3 ± 0.2	223 ± 26	22 ± 2.4	4.2 ± 3.2	37.1 ± 5.7	7.8 ± 0.5	1.69 ± 0.26	37/21
3: coral	35.2 ± 0.5	27.7 ± 0.9	350 ± 80	2.9 ± 0.5	463 ± 24	44 ± 2.4	7.0 ± 3.4	77.2 ± 6.1	8.2 ± 0.5	1.63 ± 0.11	36/22
4: coral	35.3 ± 0.6	24.7 ± 0.9	410 ± 30	3.0 ± 0.1	73 ± 12	7.0 ± 1.1	5.0 ± 4.3	12.4 ± 1.2	8.0 ± 0.5	1.76 ± 0.18	38/20
5: coral	35.3 ± 0.4	24.6 ± 0.6	380 ± 60	3.1 ± 0.4	236 ± 22	23 ± 2.1	5.2 ± 4.5	36.5 ± 6.5	8.3 ± 0.7	1.62 ± 0.29	33/18
6: coral	35.3 ± 0.3	24.5 ± 0.5	520 ± 100	2.4 ± 0.4	439 ± 9	42 ± 1.0	3.1 ± 1.7	77.1 ± 6.2	8.4 ± 0.5	1.71 ± 0.13	48/15
7: coral	35.4 ± 0.5	(22.5 ± 1.1)[a]	490 ± 30	3.0 ± 0.0	72 ± 13	6.8 ± 1.1	2.6 ± 1.7	14.2 ± 2.7	7.7 ± 0.6	2.09 ± 0.40	47/14
8: coral	35.3 ± 0.5	22.4 ± 1.1	550 ± 20	2.7 ± 0.1	220 ± 38	21 ± 3.5	1.9 ± 1.0	42.6 ± 3.1	7.7 ± 0.6	1.87 ± 0.11	26/10
9: coral	35.3 ± 0.3	22.6 ± 1.1	700 ± 30	2.1 ± 0.1	440 ± 11	43 ± 1.8	1.0 ± 0.6	77.2 ± 2.9	8.4 ± 0.4	1.78 ± 0.07	23/4
1, 4, 7: CCA	35.1 ± 0.8	Includes[d] all T treatments, 22.4–27.8	410 ± 80[d]	3.1 ± 0.2	75 ± 17	7.1 ± 1.5	nc	8.8 ± 0.8	3.5 ± 1.0	nc	3/3
2, 5, 8: CCA	35.2 ± 0.7	Includes[d] all T treatments, 22.4–27.8	415 ± 110[d]	3.0 ± 0.3	225 ± 28	22 ± 2.6	nc	13.4 ± 1.9	3.4 ± 0.7	nc	3/3
3, 6, 9: CCA	35.3 ± 0.4	Includes[d] all T treatments, 22.4–27.8	525 ± 170[d]	2.5 ± 0.5	447 ± 27	43 ± 2.7	nc	35.0 ± 9.2	5.0 ± 1.1	nc	2/2

[a] Temperature was not measured in tank 7, so temperature is the average of tanks 8 and 9, which shared the same temperature-controlled water bath.

[b] Coral Ba/Ca and K_{Ba} were calculated after correction for CCA contamination.

[c] Groups of individuals were combined for elemental analysis on samples of ≥70 μg. K_{Ba} was calculated from these combined samples. nc: not calculated for encrusting coralline algae (CCA).

[d] CCA physical parameters are averaged over tanks: 1, 4, 7 (low Ba treatment), 2, 5, 8 (medium Ba treatment) and 3, 6, 9 (high Ba treatment).

Pelletier et al., 2007) utilizing the constants of Mehrbach et al. (1973) as refit by Dickson and Millero (1987).

Each corallite, the coral skeleton, was examined under a microscope, removed from the ceramic tile and weighed on a microbalance (Cohen and Holcomb, 2009). This weight was used to calculate calcification rate over the 14-day experiment. Efforts were made to remove only the corallite, however some material from the heavily encrusted tiles adhered to the corallites, as evidenced by low Sr/Ca ratios (see discussion in Section 3.1 below). Several samples of CCA were also removed and analyzed in the same manner as coral samples. Elemental analysis was conducted on individual skeletons that weighed at least 70 μg, otherwise multiple individuals from the same tile were grouped together for analysis. Skeletal material was dissolved in 5% Optima nitric acid and analyzed via inductively coupled plasma mass spectrometry (ICP-MS) on a Finnigan Element II at the Woods Hole Oceanographic Institution ICP-MS Facility. Counts of ^{48}Ca, ^{88}Sr and ^{138}Ba were made in low-resolution mode with 45 scans per sample and a 3-minute wash in 5% nitric acid between samples. Sample counts were blank corrected with a 5% nitric acid solution. Ba/Ca and Sr/Ca elemental standards were gravimetrically prepared and used to monitor instrument drift. Three carbonate reference materials were analyzed, including two fish otolith standards (FEBS-1, Ba/Ca = 4.2 μmol mol^{-1}, Sr/Ca = 2.5 mmol mol^{-1} National Research Council Canada, and one detailed in Yoshinaga et al. (2000), Ba/Ca = 2.2 μmol mol^{-1}, Sr/Ca = 2.8 mmol mol^{-1}) and the JCp-1 coral reference standard (Ba/Ca = 7.5 μmol mol^{-1}, Sr/Ca = 8.7 mmol mol^{-1}, Okai et al. (2002)). Based on repeated standard measurements analytical uncertainty for Ba/Ca was 1 μmol mol^{-1} and for Sr/Ca, 0.5 mmol mol^{-1}.

Dissolved Ba in aliquots (filtered at 0.22 μm) from each tank in the coral culture experiment was analyzed by isotope dilution mass spectrometry (Fassett and Paulsen, 1989). Samples were diluted 25 times with 5% Optima nitric acid, spiked with ^{135}Ba and analyzed via ICP-MS for masses ^{135}Ba and ^{138}Ba in low-resolution mode with 45 scans per sample and a 3-minute rinse in 5% nitric acid. Sample counts were corrected for blanks measured in 5% nitric acid. Ca concentrations were determined with a Dionex ion chromatograph referenced to the IAPSO standard (10.5 ± 0.1 mmol kg^{-1}, n = 20). To quantify accuracy, Ba was measured in the SLRS-4 dissolved reference material (89.3 ± 1.8 nmol kg^{-1} (measured) compared to 88.8 nmol kg^{-1} (reference), n = 10). Additional reference waters without certified Ba concentrations were measured to determine analytical precision and uncertainty at higher and lower Ba concentrations: NASS-5: 45 ± 0.5 and SLEW-3: 179 ± 2, n = 10); analytical uncertainty was 2 nmol kg^{-1} based on these replicate analyses since sample Ba concentrations were greater than 70 nmol kg^{-1}.

3. RESULTS

3.1. Coral barium incorporation experiments

Conditions within the individual tanks are shown in Table 2 and Supplemental Table 1. Salinity in all tanks was ~35, with a standard deviation of 3%. The three temperature conditions (27.7, 24.6 and 22.5 °C) experienced a standard deviation of 1.1 °C over the course of the 14-day experiment. The CO_2 content and resulting aragonite saturation state is dependent on the water temperature, thus tanks at lower temperatures had slightly higher CO_2 levels and lower saturation states. This was particularly evident in Tank 9, the low temperature, high Ba tank (Table 2). Coral polyps in this tank had the lowest calcification rates (Table 2). However, in general, most tanks had a saturation state of approximately 3. The three different dissolved Ba concentrations (~73, 230 and 450 nmol kg^{-1}) were maintained in the aquaria for the length of the experiment with a standard deviation of 1–2.5 nmol kg^{-1} (Table 2, Supplementary Table 1). The resulting water Ba/Ca were 6.8–7.5, 21–23 and 42–44 μmol mol^{-1} with a standard deviation of 1–3.5 μmol mol^{-1} (Table 2).

Coral polyps grown in seawater amended with Ba incorporated this signal in their skeletal material, demonstrating a direct response to increased seawater Ba/Ca (individuals n = 325, element ratio measurements n = 164 due to analysis of some grouped individuals). However, low Sr/Ca values and a linear trend between Sr/Ca and Ba/Ca suggested that calcite from encrusting coralline algae was included in samples with the coral aragonite (Fig. 1a). Samples of CCA material with no coral skeleton present had a Sr/Ca ratio of 3.5 ± 1.0, 3.4 ± 0.7 and 5 ± 1.1 mmol mol^{-1} and Ba/Ca ratios of 8.8 ± 1.8, 13.4 ± 1.9 and 35 ± 9.2 μmol mol^{-1} for the ~73, 230 and 450 nmol kg^{-1} Ba treatment levels, respectively (Table 2). To correct for inclusion of CCA material, which would lower Ba/Ca ratios relative to pure aragonite (see mixing line in Fig. 1a), we calculated two-end member mixing between the contaminating CCA phase and aragonite. In this approach, we use Sr/Ca ratios to estimate the fraction of CCA in each sample according to:

$$f_C = \frac{Sr/Ca_M - Sr/Ca_A}{Sr/Ca_C - Sr/Ca_A} \tag{1}$$

where Sr/Ca_M, Sr/Ca_A, and Sr/Ca_C are the measured corallite, aragonite end member and CCA ratios respectively. The aragonite end member was estimated from the temperature dependence of aragonite Sr/Ca ratios:

$$Sr/Ca = 10.781 - 0.0597T \quad (Porites, \text{ [Felis etal., 2004]}) \tag{2}$$

$$Sr/Ca = 10.73 - 0.0657T \quad (Porites, \text{ [Correge etal., 2000]}) \tag{3}$$

$$Sr/Ca = 10.184 - 0.00408T \quad (Favia, \text{ [Seo etal., 2013]}) \tag{4}$$

These three Sr/Ca temperature relationships are quite different; the two Porites relationships used here were chosen since they predict coral aragonite Sr/Ca ratios that vary by 0.2 mmol mol^{-1} over the temperature range of these experiments, while the Seo et al. (2013) relationship is exclusively for the species used in these experiments (Favia). When the fraction of material contributed by CCA is calculated from Eq. (1) using aragonite Sr/Ca end member values from either Eqs. (2), (3) or (4), the difference was
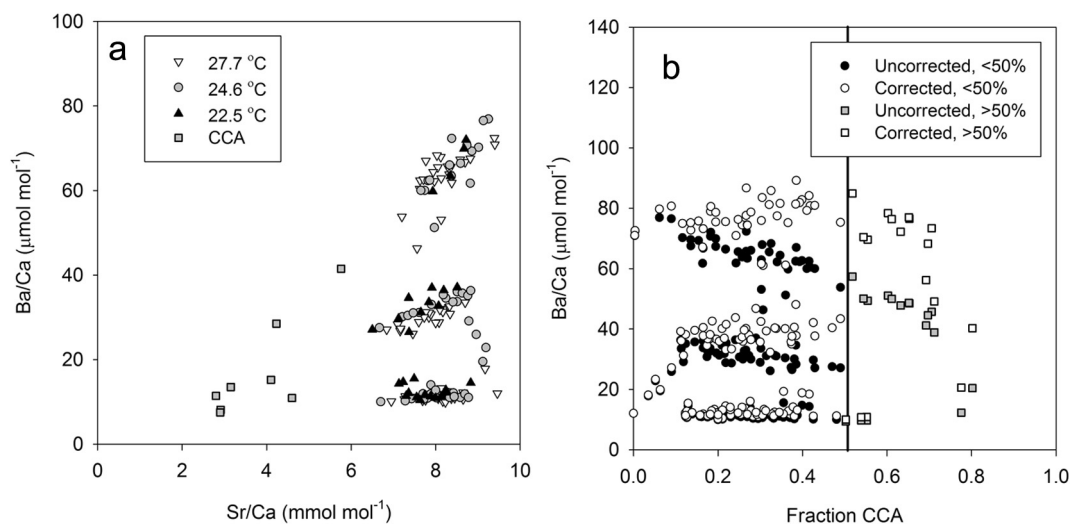
Fig. 1. (a) There is a linear relationship between Sr/Ca and Ba/Ca for the *Favia fragum* corallites that lies outside values anticipated for pure aragonite phases, suggesting mixing of a encrusting coralline algae (CCA) end member (gray squares) with aragonite. (b) Ba/Ca for uncorrected (solid symbols) and corrected (empty symbols) versus fraction CCA contribution to the sample based on two end member mixing with Sr/Ca. Samples with a CCA contribution >50 wt% (squares) were excluded from analysis.

small ($3 \pm 1\%$). In the end, we chose to include all three relationships in the uncertainty analysis to produce the most reasonable uncertainty for the fraction CCA and resulting corrected coral Ba/Ca (see below). Uncertainty associated with corrections for CCA contamination was constrained with Monte Carlo simulations (10^5 iterations) using the following uncertainties (Table 2): (1) CCA Sr/Ca measurement average and standard deviation for each treatment, (2) analytical Sr/Ca measurement uncertainty, (3) tank temperature average and standard deviation and (4) the average coral Sr/Ca for coral aragonite calculated according to Eqs. (2), (3) and (4). The simulations suggest that on average CCA contributed 30 ± 16 wt% (Fig. 1b). Samples with greater than 50 wt% CCA contribution (18 of the 164 samples, Fig. 1b and Supplemental Table 2) had very high corrected Ba/Ca and were excluded from all further analysis. Excluding those samples resulted an average CCA contribution by weight of $26 \pm 11\%$.

The same two end member mixing relationship was used to calculate the Ba/Ca ratio of the coral aragonite:

$$Ba/Ca_A = \frac{Ba/Ca_M - f_C Ba/Ca_C}{1 - f_C} \qquad (5)$$

where Ba/Ca_M is the measured ratio of the mixed coral and CCA sample, and Ba/Ca_C was 8.8 ± 1.8, 13.4 ± 1.9 and 35 ± 9.2 µmol mol^{-1} for the three Ba treatment levels. This correction assumes that CCA and aragonite have the same calcium concentration, which requires that the CCA end-member is some form of $CaCO_3$. The average increase from measured Ba/Ca to final aragonite values was 1.0 ± 0.8 µmol mol^{-1} ($9 \pm 6\%$), 6.7 ± 3.6 µmol mol^{-1} ($22 \pm 12\%$), and 11.9 ± 6.2 µmol mol^{-1} ($19 \pm 10\%$) for low, medium and high Ba treatments respectively (Fig. 1b). Once again, the temperature dependence of the Sr/Ca ratio did not have a large impact on the resulting Ba/Ca (1.0 ± 0.9 µmol mol^{-1} difference between Eq. (3) and (4) for all 148 samples). We used Monte Carlo simulations to determine the uncertainty in corrected coral Ba/Ca, as discussed above, including these additional sources of uncertainty: (1) CCA Ba/Ca measurement average and standard deviation for each treatment and (2) analytical Ba/Ca measurement uncertainty. Corrected coral Ba/Ca averaged 12.7 ± 2.0, 38.0 ± 6.0 and 77.2 ± 5.8 µmol mol^{-1} at the three dissolved Ba concentrations (Fig. 2). While this correction is important, it does not change the conclusion that corals incorporate Ba linearly over this seawater Ba range.

The corallite calcification rate exhibited a temperature dependence, with higher calcification rates observed at higher temperatures ($n = 325$, Fig. 3a). Inclusion of CCA material attached to the coral skeleton will result in calcification rates that are too large, so the same correction was done as above to remove the contribution of this material prior to calculating calcification rates. Since the correction could only be done for samples with measured Sr/Ca ratios, when multiple individuals were grouped for a single analysis, the weighted calcification rate of that composite sample was corrected for CCA inclusion. We exclude samples with >50 wt% CCA. All further discussion and analysis is based on these samples ($n = 148$, Fig. 2b–d). In addition to the diminished metabolic response at lower temperatures, these tanks also had a lower saturation state since CO_2 is more soluble in water at 22.5 versus 27.7 °C. Calcification is inhibited at lower saturation states. The range in calcification rates for individual polyps was quite large, with the majority of specimens in the warm tanks (27.7 °C) having calcification rates between 4.2 and 7.0 mg $CaCO_3$ d^{-1}, while rates in the cool tanks (22.5 °C) fell between 1.0 and 2.6 mg d^{-1} (Fig. 3 and Table 2). The lowest calcification rates were also coincident with the lowest saturation states, particularly for tanks 9, 8 and 6, although there was no statistical difference (two-way factorial ANOVA test, $p > 0.1$) between saturation states at the different treatments.
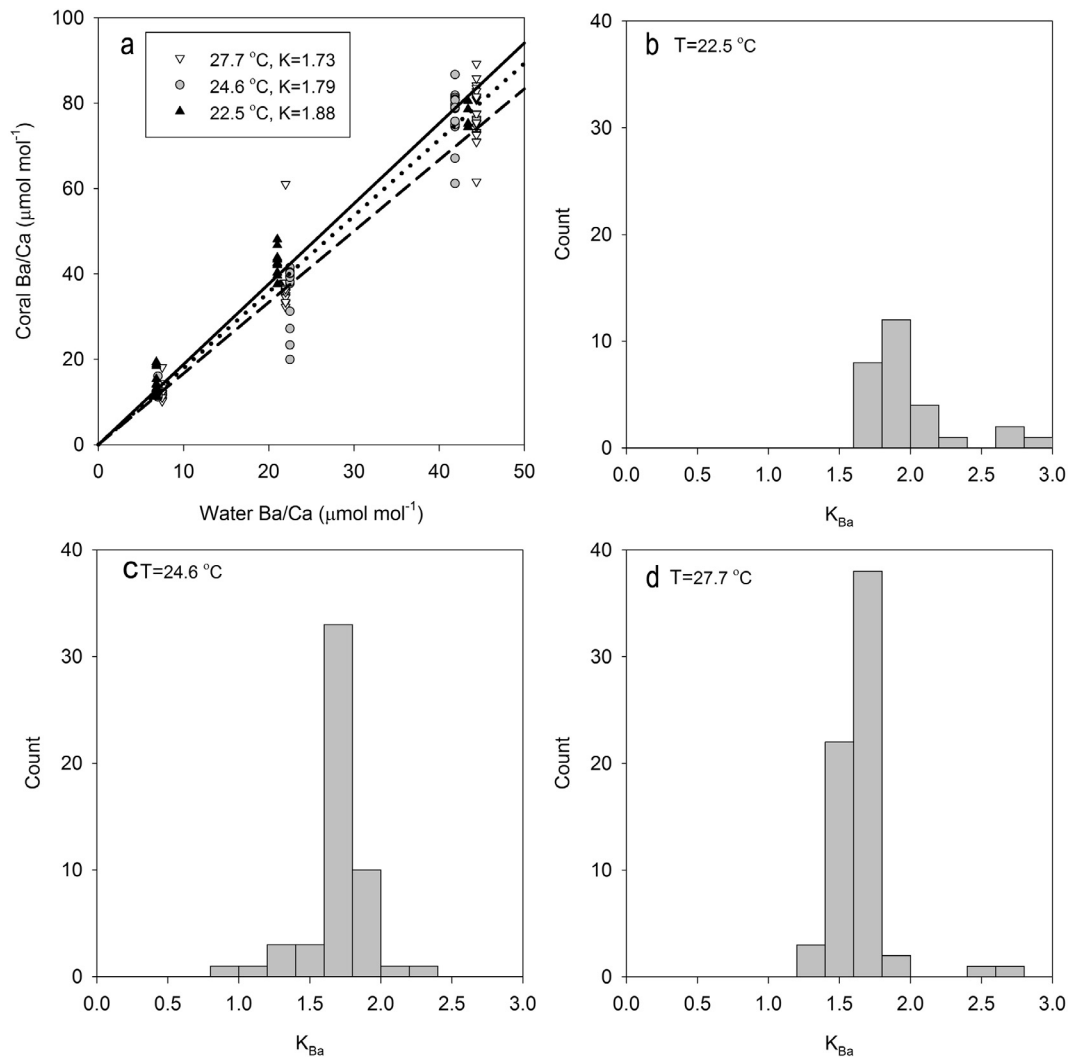
Fig. 2. (a) Coral Ba/Ca versus water Ba/Ca for *Favia fragum* polyps grown in barium amended aquaria at three different temperatures. Best-fit lines are solid ($T = 22.5$ °C), dotted ($T = 24.6$ °C) and dashed ($T = 27.7$ °C). These lines were fit through the origin and the slopes yield the experiment distribution coefficient, K. Histogram of individual distribution coefficients for (b) $T = 22.5$ °C, (c) $T = 24.6$ °C and (d) $T = 27.7$ °C, 11 bins for each temperature treatment.

4. DISCUSSION

4.1. Coral Ba uptake

The distribution coefficient describes the partitioning of Ba between solid aragonite and dissolved phases according to:

$$K_{Ba} = \frac{Ba/Ca_{argonite}}{Ba/Ca_{dissolved}} \qquad (6)$$

The distribution coefficient must be constrained to quantitatively use coral Ba/Ca as an environmental paleo proxy of ocean water chemistry. Experimental results indicate the corals incorporate Ba in direct proportion to the seawater dissolved Ba across a large concentration range (72–463 nmol kg^{-1}). To our knowledge, this is the first time the concentration response of Ba uptake into coral aragonite has been demonstrated experimentally. Our results

are consistent with those observed for other marine species (calcite foraminifera, Lea and Spero, 1992; and aragonitic fish otoliths, Bath et al., 2000; Elsdon and Gillanders, 2003). However, there is large variability in individual Ba uptake efficiency resulting in variable distribution coefficients (Figs. 2 and 4). Below we consider the potential impact of temperature, calcification rate, and aragonite saturation state on this inter-specimen variability.

4.2. Coral Ba/Ca distribution coefficient

4.2.1. Temperature dependence of K_{Ba}

Experiments with inorganic aragonite over large temperature ranges (10–75 °C) show that K_{Ba} is inversely related to temperature (Dietzel et al., 2004; Gaetani and Cohen, 2006), such that aragonite precipitated at a lower temperature will have a higher Ba/Ca (Fig. 4a). There is a large range in skeletal Ba/Ca, as discussed above. To evaluate
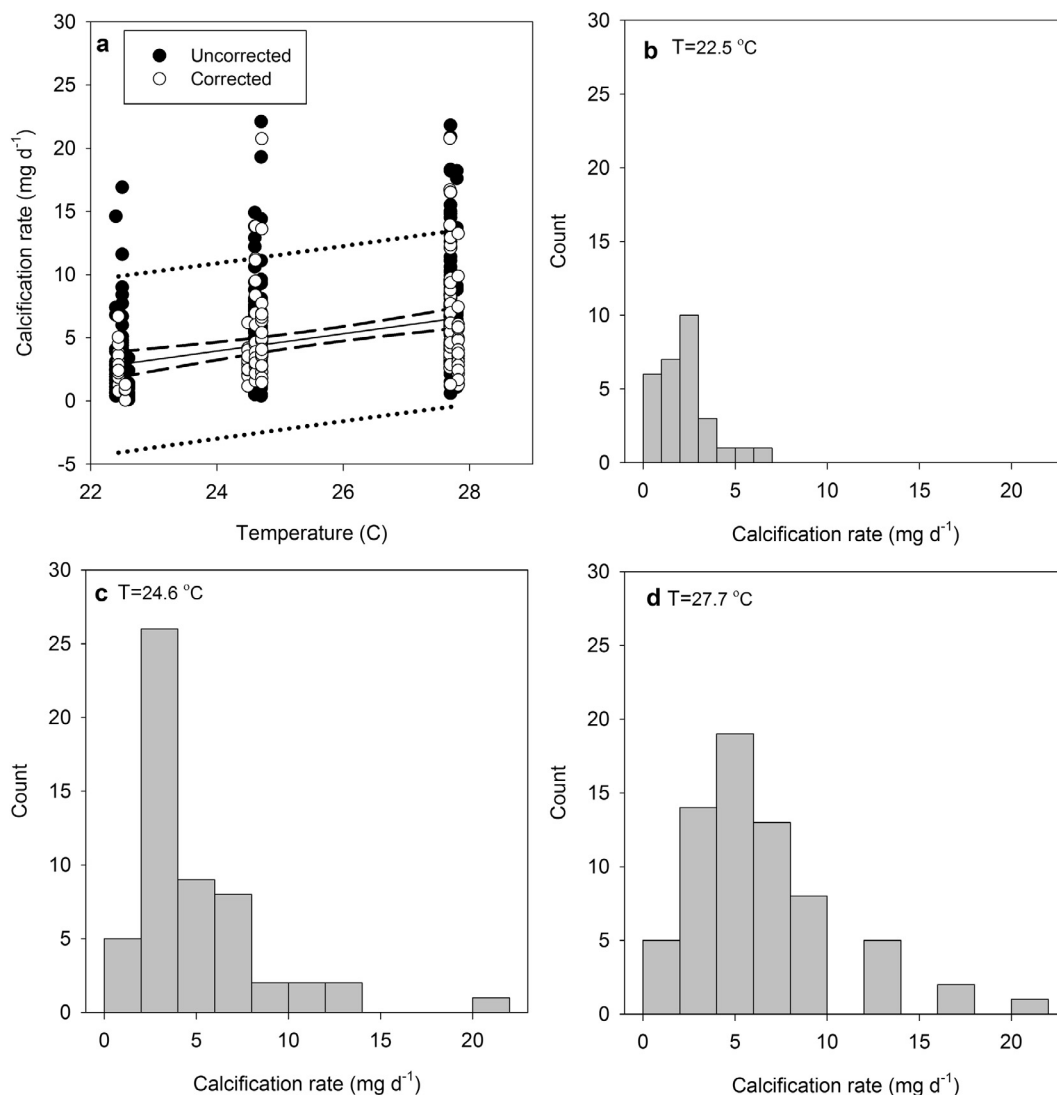
Fig. 3. (a) Coral calcification rate for uncorrected (solid) and CCA corrected (empty) versus temperature. Data at each temperature includes polyps from each of the three different Ba treatments. The best-fit line (solid) is shown for the relationship: coral calcification rate = 0.68 × temperature − 12.29 (T in °C, $r^2 = 0.14$, $p < 0.0001$); dashed lines indicate the 95% confidence interval, while dotted line represents 95% prediction interval. Histograms of corrected calcification rate for each temperature treatment are shown in (b) $T = 22.5$ °C, (c) $T = 24.6$ °C and (d) $T = 27.7$ °C. Precipitation rates from each treatment were grouped into an equal number of bins (11) in the histograms, corresponding to different bin ranges for each temperature.

the influence of temperature on Ba partitioning, the distribution coefficient at each experimental temperature was calculated from the regression slope between coral and water Ba/Ca with an intercept set at zero. The choice of Sr/Ca temperature dependence for the CCA correction results in a maximum change of 0.1 in the K_{Ba}. This represents approximately 5% and 6% of the low and high temperature average K_{Ba}, respectively, and is similar to the K_{Ba} standard error, as calculated from the linear regressions. In these experiments, the distribution coefficients were: 27.7 °C, $K_{Ba} = 1.73$ (1.69–1.77, 95% confidence interval (CI)), at 24.6 °C, $K_{Ba} = 1.79$ (1.73–1.84, 95% CI) and at 22.5 °C, $K_{Ba} = 1.88$ (1.81–1.95, 95%CI). The 95% confidence intervals overlap due to the large range in polyp Ba/Ca. Lea et al. (1989) report lower K_{Ba} values for mature colo-

nies of *Diploria labyrinthiformis* (Bermuda) and *Montastrea annularis* (Bermuda) ($K_{Ba} = 1.27 \pm 0.03$) and for *Pavona Clavus* (Galapagos) ($K_{Ba} = 1.41 \pm 0.14$). The temperature dependence of the distribution coefficient for the *F. fragum* polyps falls along this regression line (Fig. 4a):

$$K_{Ba} = 2.514 \pm 0.190 - 0.02865 \pm 0.01487T \qquad (7)$$

where T is temperature in °C. The experimentally precipitated inorganic aragonite in Gaetani and Cohen (2006) displays a greater temperature dependence than we observe for the *Favia* polyps or reported in Dietzel et al. (2004) (also in DeCarlo et al. (2015); see discussion below). Over the temperature range used in these experiments (22.5–27.7 °C), Dietzel et al. (2004) predicts a decrease in K_{Ba} of 0.19, DeCarlo et al. (2015) predicts a 0.22 decrease, and
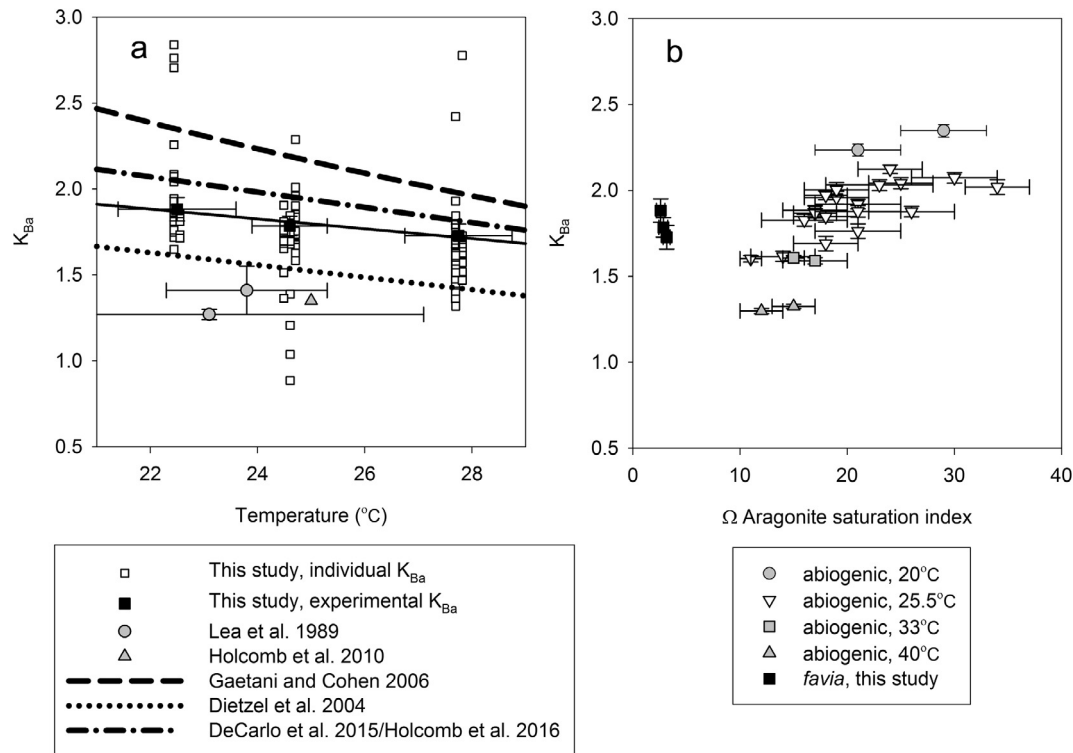
Fig. 4. (a) Temperature dependence of the Ba distribution coefficient (K_{Ba}) for the *Favia fragum* corallites grown in culture as well as three abiogenic K_{Ba} temperature dependences. Values for Lea et al. (1989) *M. annularis* (Bermuda) and *P. Clavus* (Galapagos) are also shown. For this experiment, K_{Ba} at each temperature was calculated from the slope of corrected coral Ba/Ca versus water Ba/Ca; K_{Ba} error bars are the 95% confidence interval for the slope and temperature error bars represent the standard deviation during the experiment. K_{Ba} calculated for each individual is also shown. The best-fit line (solid) is shown for the experimental distribution coefficient-temperature relationship: $K_{Ba} = 2.514 - 0.02865T$ (T in °C). (b) Abiogenic aragonite K_{Ba} values vary as a function of aragonite saturation state (data from DeCarlo et al. (2015) and Holcomb et al. (2016) as described in the text). The *F. fragum* K_{Ba} fall off this relationship, likely as a result of modification of calcifying fluid, as saturation state is shown for the bulk aquaria water.

Gaetani and Cohen (2006) predict a decrease of 0.37, compared to the 0.15 reduction that we observe in the *Favia* experiment.

4.2.2. Precipitation rate and aragonite saturation state influence on K_{Ba}

In addition to temperature, elemental partitioning in aragonite has been related to other variables, such as calcification rate (Reynaud et al., 2007), extension rate (Pingitore et al., 1989; Saenger et al., 2008), aragonite saturation state (Kleypas et al., 1999; DeCarlo et al., 2015), and Rayleigh fractionation (Gaetani and Cohen, 2006). In these experiments, calcification rate, temperature, and aragonite saturation index are linked since we observed an increase in calcification at higher temperatures and saturation states, as reported previously (*F. fragum*, Barkley, 2011; *Stylophora pistillata*, Reynaud et al., 2003; *Cladocora caespitosa*, Rodolfo-Metalpa et al., 2008), although evidence has been presented elsewhere for a decline in calcification at the highest temperature used in these experiments (27.7 °C, *Galaxea fascicularis* and *Dendrophyllia*, Marshall and Clode, 2004). This increase in calcification at higher temperatures is potentially due to higher efficiency in the enzyme-regulated processes associated with calcification at

increased temperatures, although species dependence cannot be ruled out (Marshall and Clode, 2004).

K_{Ba} has been shown to increase concurrent with precipitation rates (Cohen and Gaetani, 2010). To explore the potential impact of calcification rate on Ba partitioning, we can compare the *F. fragum* experiment results to inorganic aragonite precipitation experiments (Dietzel et al., 2004; Gaetani and Cohen, 2006; Holcomb et al., 2010). In this study, the K_{Ba} was calculated for each individual or grouped sample (see Methods) and compared to the calcification rate determined for that individual or grouped sample. In addition, we calculated K_{Ba} from the abiogenic experiments described in DeCarlo et al. (2015) and Holcomb et al. (2016). We did this by using the measurements of the aragonite Ba/Ca from Holcomb et al. (2016), the fluid [Ca] from DeCarlo et al. (2015), the local seawater Ba/Ca from Gaetani and Cohen (2006), and following the partitioning calculations described in DeCarlo et al. (2015).

The coral K_{Ba} values reported here are higher than those determined for inorganic aragonite reported by Dietzel et al. (2004) and Holcomb et al. (2010), but less than the values predicted by Gaetani and Cohen (2006) or calculated from DeCarlo et al. (2015) and Holcomb et al. (2016)

(Fig. 4a). These experiments induced precipitation by creating supersaturated conditions with respect to aragonite. The experimental study design resulted in varying precipitation rates for each study: Dietzel et al., 2004 reports ~10 mg d^{-1}, 40–70 mg d^{-1} reported by Gaetani and Cohen (2006) and DeCarlo et al. (2015) ranged from 50 to 500 mg d^{-1} (170 average). The growth rate in the Holcomb et al. experiment is not reported, although Cohen and Gaetani (2010) indicate that it was lower than 40–70 mg d^{-1}. In this study, precipitation rates for *F. fragum* in each treatment averaged from 1 to 7 mg d^{-1}. Precipitation rate does not appear to explain the higher K_{Ba} reported here compared to the abiogenic experiments. Note that while precipitation rate and distribution coefficient are both correlated to temperature in this experiment, there is no correlation between calcification rate and K_{Ba} ($r^2 = 0.01$). While it is possible the range in precipitation rates in the current culture experiments is too small compared to the individual polyp variability to discern a precipitation rate dependence on K_{Ba}, calcification rate does not appear to drive changes in K_{Ba}.

Coral biomineralization processes may drive Ba/Ca variability in our experiments. Corals precipitate their skeletons from a calcifying fluid that is supplied by seawater, but is isolated, or semi-isolated, with respect to the external seawater environment (Cohen and McConnaughey, 2003; Venn et al., 2011; Gagnon et al., 2012). Precipitation of aragonite from an isolated reservoir modifies the elemental composition of the calcifying fluid by raising pH, effectively elevating the aragonite saturation state (Al-Horani et al., 2003; Venn et al., 2013). During this process, elements with $K_i > 1$ (such as Ba) are depleted relative to Ca in the coral calcifying fluid as precipitation proceeds from an isolated reservoir of fluid. Greater precipitation rates will therefore decrease the Ba/Ca ratio of the calcifying fluid and the Ba/Ca ratio of the coral skeleton precipitated from the fluid. Gaetani et al. (2011) described this as a Rayleigh fractionation process and found that the mass fraction of aragonite precipitated from the fluid increases (*i.e.* greater extent of precipitation) with increasing temperature. In addition, abiotic aragonite experiments have shown an increase in K_{Ba} with increasing aragonite saturation state (Fig. 4b, Supplemental Table 3: K_{Ba} calculated according to DeCarlo et al. (2015) from fluid [Ca] (DeCarlo et al., 2015), dissolved Ba/Ca ratio (Gaetani and Cohen, 2006), and aragonite Ba/Ca (Holcomb et al., 2016)). The *F. fragum* results fall off of the inorganic relationship, though, however saturation state is reported for the bulk seawater, not the calcifying fluid, which is likely higher. Variability in calcifying fluid chemistry and precipitation efficiency could potentially explain the large variability in coral Ba/Ca and individual K_{Ba} seen here, as well as contribute to the temperature dependence of K_{Ba} that we observed. However, these influences cannot be resolved in this study.

5. IMPLICATIONS FOR CORAL BA/CA AS A PALEOPROXY

Through coral culture work we have shown that corals incorporate Ba in direct proportion to seawater concentrations up to >400 nmol kg^{-1}. Based on the distribution coef-

ficient temperature dependence found here, the potential influence of temperature on coral Ba/Ca ratios from 20 to 28 °C in constant coastal ocean Ba concentrations of 50 nmol kg^{-1} would be 1.1 μmol mol^{-1}, or ~13% increase corresponding to cooler temperatures. Peak Ba/Ca ratios have been reported that are much greater than this, for example peak values of 12–17 μmol mol^{-1}, attributed to river discharge to the Great Barrier Reef (Sinclair and McCulloch, 2004); 6–15 μmol mol^{-1} attributed to upwelling in the Red Sea (Tudhope et al., 1996); and 8–18 μmol mol^{-1}, attributed to sediment input in Hawaii (Prouty et al., 2010) (see Table 1). The partition coefficient temperature dependence is not sufficient to explain such large coral Ba/Ca peaks. If these increases in coral Ba/Ca are due primarily to changes in water chemistry, then elevated coastal ocean Ba concentrations must be sustained over the time period that corresponds to coral calcification. There is less evidence for large, temporally-sustained coastal ocean Ba concentrations of 80–140 nmol kg^{-1}, or higher, to support the large coral Ba/Ca peaks identified in Table 1. Typical coastal ocean Ba range from 40 to 75 nmol kg^{-1}, and are dependent on external dissolved Ba inputs and water residence times (Shaw et al., 1998; Gonnea et al., 2014). In addition, oceanic Ba cycling between the dissolved and particulate phase is controlled in part by productivity through precipitation of barite (BaSO$_4$) in decomposing organic matter and ultimately burial in sediments (Dehairs et al., 1980; Ganeshram et al., 2003). However, it is unlikely that this process will modify coastal ocean Ba concentrations to sufficiently explain the commonly observed annual cycle in coral Ba/Ca. Finally, the organic matter associated with the coral polyp is highly enriched in Ba, which is removed prior to analysis through oxidation of sample material (Lea and Boyle, 1993). While there is some evidence that organic matter is preserved within the skeleton (Ingalls et al., 2003), it is not known if this organic matter contributes to coral skeletal Ba/Ca below the polyp layer. Given the current uncertainty in how Rayleigh fractionation, calcification rate, extension rate, and saturation state affect coral Ba/Ca ratios, relating coral Ba/Ca paleo records to changes in seawater Ba/Ca should be approached with caution. Finally, it is necessary to quantify natural variability in ocean Ba concentrations across appropriate temporal scales in response to the various environmental conditions for which Ba has been invoked as a useful tracer.

APPENDIX A. SUPPLEMENTARY MATERIAL

Supplementary data associated with this article can be found, in the online version, at http://dx.doi.org/10.1016/j.gca.2017.04.006.

REFERENCES

Al-Horani F. A., Al-Moghrabi S. M. and De Beer D. (2003) The mechanism of calcification and its relation to photosynthesis and respiration in the scleractinian coral *Galaxea fascicularis*. *Mar. Biol.* **142**, 419–426.

Alibert C. and Kinsley L. (2008) A 170-year Sr/Ca and Ba/Ca coral record from the western Pacific warm pool: 1. What can we learn from an unusual coral record? *J. Geophys. Res.-Oceans* **113**. http://dx.doi.org/10.1029/2006jc003979.

Alibert C., Kinsley L., Fallon S. J., McCulloch M. T., Berkelmans R. and McAllister F. (2003) Source of trace element variability in Great Barrier Reef corals affected by the Burdekin flood plumes. *Geochim. Cosmochim. Acta* **67**, 231–246.

Barkley H. C. (2011) *Establishing Links Between Basin-scale Climate and the Growth of Atlantic Corals: The Effect of Temperature and Feeding on Favia fragum*. Ecology and Evolutionary Biology Department, Princeton University, p. 96.

Bath G. E., Thorrold S. R., Jones C. M., Campana S. E., McLaren J. W. and Lam J. W. H. (2000) Strontium and barium uptake in aragonitic otoliths of marine fish. *Geochim. Cosmochim. Acta* **64**, 1705–1714.

Busenberg E. and Plummer L. N. (1986) A comparative study of the dissolution and crystal growth kinetics of calcite and aragonite. In *Studies in Diagenesis*, vol. 1578 (ed. F. A. Mumpton). U.S. Geological Survey Bulletin, pp. 139–168.

Carriquiry J. D. and Horta-Puga G. (2010) The Ba/Ca record of corals from the Southern Gulf of Mexico: contributions from land-use changes, fluvial discharge and oil-drilling muds. *Mar. Pollut. Bull.* **60**, 1625–1630.

Chen T. R., Yu K. F., Li S., Chen T. G. and Shi Q. (2011) Anomalous Ba/Ca signals associated with low temperature stresses in Porities corals from Daya Bay, northern South Cina Sea. *J. Environ. Sci.* **23**, 1452–1459.

Cohen A. L. and Gaetani G. A. (2010) Ion partitioning and the geochemistry of coral skeletons: solving the mystery of the "Vital Effect". In *On Partitioning in Low Temperature Aqueous Systems: From Fundamentals to Applications in Climate Proxies and Environmental Geochemistry* (eds. M. Prieto and H. Stoll). European Mineralogical Union, Notes in Mineralogy.

Cohen A. L. and Holcomb M. (2009) Why corals care about ocean acidification: uncovering the mechanism. *Oceanography* **22**, 118–127.

Cohen A. L. and McConnaughey T. A. (2003) Geochemical perspectives on coral mineralization. *Rev. Mineral. Geochem.* **54**, 151–187.

Corrége T., Delcroix T., Recy J., Beck W., Cabioch G. and Le Cornec F. (2000) Evidence for stronger El Nino-Southern Oscillation (ENSO) events in a mid-Holocene massive coral. *Paleoceanography* **15**, 465–470.

de Putron S. J., McCorkle D. C., Cohen A. L. and Dillon A. B. (2011) The impact of seawater saturation state and bicarbonate ion concentration on calcification by new recruits of two Atlantic corals. *Coral Reefs* **30**, 321–328.

DeCarlo T. M., Gaetani G. A., Holcomb M. and Cohen A. L. (2015) Experimental determination of factors controlling U/Ca of aragonite precipitated from seawater: Implications for interpreting coral skeleton. *Geochim. Cosmochim. Acta* **162**, 151–165.

Dehairs F., Chesseleet R. and Jedwab J. (1980) Discrete suspended particles of barite and the barium cycling in the open ocean. *Earth Planet. Sci. Lett.* **49**, 528–550.

Dickson A. and Millero F. (1987) A comparison of the equilibrium constants for the dissociation of carbonic acid in seawater media. *Deep Sea Res. Part A* **34**, 1733–1743.

Dietzel M., Gussone N. and Eisenhauer A. (2004) Co-precipitation of Sr^{2+} and Ba^{2+} with aragonite by membrane diffusion of CO_2 between 10 and 50 °C. *Chem. Geol.* **203**, 139–151.

Drenkard E. J., Cohen A. L., McCorkle D. C., de Putron S. J., Starczak V. R. and Zicht A. E. (2013) Calcification by juvenile corals under heterotrophy and elevated CO_2. *Coral Reefs*. http://dx.doi.org/10.1007/s00338-00013-01021-00335.

Elsdon T. S. and Gillanders B. M. (2003) Relationship between water and otolith elemental concentrations in juvenile black bream *Acanthopagrus butcheri*. *Mar. Ecol. Prog. Ser.* **260**, 263–272.

Fallon S. J., McCulloch M. T., van Woesik R. and Sinclair D. J. (1999) Corals at their latitudinal limits: laser ablation trace element systematics in Porites from Shirigai Bay, Japan. *Earth Planet. Sci. Lett.* **172**, 221–238.

Fassett J. D. and Paulsen P. J. (1989) Isotope dilution mass spectrometry for accurate elemental analysis. *Anal. Chem.* **61**, 643A–649A.

Felis T., Lohmann G., Kuhnert H., Lorenz S. J., Scholz D., Patzold J., Al-Rousan S. A. and Al-Moghrabi S. M. (2004) Increased seasonality in Middle East temperatures during the last interglacial period. *Nature* **429**, 164–168.

Fleitmann D., Dunbar R. B., McCulloch M., Mudelsee M., Vuille M., McClanahan T. R., Cole J. E. and Eggins S. (2007) East African soil erosion recorded in a 300 year old coral colony from Kenya. *Geophys. Res. Lett.* **34**. http://dx.doi.org/10.1029/2006gl028525.

Gaetani G. A. and Cohen A. L. (2006) Element partitioning during precipitation of aragonite from seawater: a framework for understanding paleoproxies. *Geochim. Cosmochim. Acta* **70**, 4617–4634.

Gaetani G. A., Cohen A. L., Wang Z. and Crusius J. (2011) Rayleigh-based, multi-element coral thermometry: a biomineralization approach to developing climate proxies. *Geochim. Cosmochim. Acta* **75**, 1920–1932.

Gagnon A. C., Adkins J. F. and Erez J. (2012) Seawater transport during coral biomineralization. *Earth Planet. Sci. Lett.* **329**, 150–161.

Gaillardet J., Viers J. and Dupre B. (2003) 5.09 - Trace elements in river waters. In *Treatise on Geochemistry* (eds. D. H. Heinrich and K. T. Karl). Pergamon, Oxford, pp. 225–272.

Ganeshram R. S., François R., Commeau J. and Brown-Leger S. L. (2003) An experimental investigation of barite in seawater. *Geochim. Cosmochim. Acta* **67**, 2599–2605.

Gonneea M. E., Charette M. A., Liu Q., Herrera-Silveira J. A. and Morales-Ojeda S. M. (2014) Trace element geochemistry of groundwater in a karst subterranean estuary (Yucatan Peninsula, Mexico). *Geochim. Cosmochim. Acta* **132**, 31–49.

Goodbody-Gringley G. and de Putron S. J. (2009) Planulation patterns of the brooding coral *Favia fragum* (Esper) in Bermuda. *Coral Reefs* **28**, 959–963.

Holcomb M. C., McCorkle D. C. and Cohen A. L. (2010) Long-term effects of nutrient and CO_2 enrichment on the temperate coral *Astrangia poculata* (Ellis and Solander 1786). *J. Exp. Mar. Biol. Ecol.* **286**, 27–33.

Holcomb M. C., DeCarlo T. M., Gaetani G. A. and McCulloch M. (2016) Factors affection B/Ca ratios in synthetic aragonite. *Chem. Geol.* **437**, 67–76.

Horta-Puga G. and Carriquiry J. D. (2012) Coral Ba/Ca molar ratios as a proxy of precipitation in the northern Yucatan Peninsula, Mexico. *Appl. Geochem.* **27**, 1579–1586.

Ingalls A. E., Lee C. and Druffel E. R. M. (2003) Preservation of organic matter in mound-forming coral skeletons. *Geochim. Cosmochim. Acta* **67**(2827), 2827–2841.

Jupiter S., Roff G., Marion G., Henderson M., Schrameyer V., McCulloch M. and Hoegh-Guldberg O. (2008) Linkages between coral assemblages and coral proxies of terrestrial exposure along a cross-shelf gradient on the southern Great Barrier Reef. *Coral Reefs* **27**, 887–903.

Kleypas J. A., Buddemeier R. W., Archer D., Gattuso J. P., Langdon C. and Opdyke B. N. (1999) Geochemical consequences of increased atmospheric carbon dioxide on coral reefs. *Science* **284**, 118–120.

Lea D. W. and Boyle E. A. (1993) Determination of carbonate-bound barium in foraminifera and corals by isotope dilution plasma-mass spectrometry. *Chem. Geol.* **103**, 73–84.

Lea D. W. and Spero H. J. (1992) Experimental-determination of barium uptake in shells of the planktonic-foraminifera *Orbulina-universa* at 22 °C. *Geochim. Cosmochim. Acta* **56**, 2673–2680.

Lea D. W., Shen G. T. and Boyle E. A. (1989) Coralline barium records temporal variability in Equatorial Pacific upwelling. *Nature* **340**, 373–376.

Lewis, E., Wallace, D., 1998. Program developed for CO2 system calculations. ORNL/CDIAC-105, Carbon Dioxide Information Analysis Center Oak Ridge Natl Lab. US Dept of Energy, Oak Ridge, TN.

Marshall A. T. and Clode P. (2004) Calcification rate and the effect of temperature in a zooxanthellate and an azooxanthellate scleractinian reef coral. *Coral Reefs* **23**, 218–224.

McCulloch M., Fallon S., Wyndham T., Hendy E., Lough J. and Barnes D. (2003) Coral record of increased sediment flux to the inner Great Barrier Reef since European settlement. *Nature* **421**, 727–730.

Mehrbach C., Culberso C. H., Hawley J. E. and Pytkowicx R. M. (1973) Measurement of apparent dissociation-constants of carbonic-acid in seawater at atmospheric-pressure. *Limnol. Oceanogr.* **18**, 897–907.

Montaggioni L. F., Le Cornec F., Corrége T. and Cabioch G. (2006) Coral barium/calcium record of mid-Holocene upwelling activity in New Caledonia, South-West Pacific. *Paleogeogr. Paleoclimatol. Paleoecol.* **237**, 436–455.

Moyer R. P., Grottoli A. G. and Olesik J. W. (2012) A multiproxy record of terrestrial inputs to the coastal ocean using minor and trace elements (Ba/Ca, Mn/Ca, Y/Ca) and carbon isotopes (δC-13, ΔC-14) in a nearshore coral from Puerto Rico. *Paleoceanography* **27**. http://dx.doi.org/10.1029/2011pa002249.

Okai T., Suzuki A., Kawahata H., Terashima S. and Imai N. (2002) Preparation of a new Geological Survey of Japan geochemical reference material: Coral JCp-1. *Geostand. Newsl.* **26**, 95–99.

Pelletier, G., Lewis, E., Wallace, D., 2007. CO2sys.xls: A Calculator for the CO$_2$ System in Seawater for Microsoft Excel/VBA. Washington State Department of Ecology/Brookhaven National Laboratory, Olympia, WA/Upton, NY, USA.

Pingitore N. E., Rangel Y. and Kwarteng A. (1989) Barium variation in *Acropora-palmata* and *Montastrea-annularis*. *Coral Reefs* **8**, 31–36.

Prouty N. G., Field M. E., Stock J. D., Jupiter S. D. and McCulloch M. (2010) Coral Ba/Ca records of sediment input to the fringing reef of the southshore of Moloka'i, Hawai'i over the last several decades. *Mar. Pollut. Bull.* **60**, 1822–1835.

Reuer M. K., Boyle E. A. and Cole J. E. (2003) A mid-twentieth century reduction in tropical upwelling inferred from coralline trace element proxies. *Earth Planet. Sci.* **210**, 437–452.

Reynaud S., Leclercq N., Romaine-Lioud S., Ferrier-Pages C., Jaubert J. and Gattuso J. P. (2003) Interacting effects of CO$_2$ partial pressure and temperature on photosynthesis and calcification in a scleractinian coral. *Glob. Change Biol.* **9**, 1660–1668.

Reynaud S., Ferrier-Pages C., Meibom A., Mostefaoui S., Mortlock R., Fairbanks R. and Allemand D. (2007) Light and temperature effects on Sr/Ca and Mg/Ca ratios in the scleractinian coral *Acropora* sp.. *Geochim. Cosmochim. Acta* **71**, 354–362.

Rodolfo-Metalpa R., Peirano A., Houlbreque F., Abbate M. and Ferrier-Pages C. (2008) Effects of temperature, light and heterotrophy on the growth rate and budding of the temperate coral *Cladocora caespitosa*. *Coral Reefs* **27**, 17–25.

Saenger C., Cohen A. L., Oppo D. W. and Hubbard D. (2008) Interpreting sea surface temperature from strontium/calcium ratios in Montastrea corals: link with growth rate and implications for proxy reconstructions. *Paleoceanography* **23**. http://dx.doi.org/10.1029/2007pa001572.

Seo I., Lee Y. I., Watanabe T., Yamano H., Shimamura M., Yoo C. M. and Hyeong K. (2013) A skeletal Sr/Ca record preserved in *Dipsastraea (Favia) speciosa* and implications for coral Sr/Ca thermometry in mid-latitude regions. *Geochem. Geophys. Geosyst.* **14**, 2873–2885.

Shaw T. J., Moore W. S., Kloepfer J. and Sochaski M. A. (1998) The flux of barium to the coastal waters of the southeastern USA: the importance of submarine groundwater discharge. *Geochim. Cosmochim. Acta* **62**, 3047–3054.

Sinclair D. J. (2005) Non-river flood barium signals in the skeletons of corals from coastal Queensland, Australia. *Earth Planet. Sci. Lett.* **237**, 354–369.

Sinclair D. J. and McCulloch M. T. (2004) Corals record low mobile barium concentrations in the Burdekin River during the 1974 flood: evidence for limited Ba supply to rivers? *Paleogeogr. Paleoclimatol. Paleoecol.* **214**, 155–174.

Tudhope A. W., Lea D. W., Shimmield G. B., Chilcott C. P. and Head S. (1996) Monsoon climate and Arabian sea coastal upwelling recorded in massive corals from southern Oman. *Palaios* **11**, 347–361.

Venn A., Tambutté E., Holcomb M., Allemand D. and Tambutté S. (2011) Live tissue imaging shows reef corals elevate pH under their calcifying tissue relative to seawater. *PLoS ONE* **6**, e20013. http://dx.doi.org/10.1371/journal.pone.0020013.

Venn A. A., Tambutté E., Holcomb M., Laurent J., Allemand D. and Tambutté S. (2013) Impact of seawater acidification on pH at the tissue-skeleton interface and calcification on coral reefs. *Geochim. Cosmochim. Acta* **68**, 1473–1488.

Wyndham T., McCulloch M., Fallon S. and Alibert C. (2004) High-resolution coral records of rare earth elements in coastal seawater: biogeochemical cycling and a new environmental proxy. *Geochim. Cosmochim. Acta* **68**, 2067–2080.

Yoshinaga J., Nakama A., Morita M. and Edmonds J. S. (2000) Fish otolith reference material for quality assurance of chemical analyses. *Mar. Chem.* **69**, 91–97.

Associate editor: Daniel Sinclair